Hadronic contribution to the Muon $g-2$ with emphasis on photon-photon fusion processes

Xiu-Lei Ren[1,*]

[1]Helmholtz-Institut Mainz, D-55099 Mainz, Germany

Abstract. The current status of muon $g-2$ is briefly reviewed, particularly for its hadronic contributions, hadronic vacuum polarization (HVP) and hadronic light-by-light (HLbL), using the data-driven and dispersive approach. As the subprocess of HLbL, the photon-photon fusion to hadrons, especially to $\pi^+\pi^-\pi^0$ process, is studied in detail.

1 Introduction

Most recently, the Fermilab experiment (FNAL-E989) reported their second/third phase result of the muon $g-2$ [1], which leads to a relative small uncertainty at the level of 0.2 ppm. By combining their first phase result [2] and previous Brookhaven's result [3], the updated experimental average value comes to

$$a_\mu(\text{Exp}) = 116\,592\,059(22) \times 10^{-11}, \tag{1}$$

with the unprecedented precision (~ 0.19 ppm). In comparison with the value of a_μ from the Standard Model (SM),

$$a_\mu(\text{SM}) = 116\,591\,810(43) \times 10^{-11}, \tag{2}$$

given in the Muon $g-2$ Theory Initiative white paper [4], the deviation is enlarged from $4.2\,\sigma$ to $5.1\,\sigma$. This makes the $(g-2)_\mu$ being the most possible hint of new physics beyond SM.

The SM prediction of a_μ involves the contributions from quantum electrodynamics (QED), electroweak (EW), and hadronic interactions,

$$a_\mu(\text{SM}) = a_\mu^{\text{QED}} + a_\mu^{\text{EW}} + a_\mu^{\text{Had.}}, \tag{3}$$

where QED provides more than 99.99% of the total value with negligible uncertainty. Conversely, the hadronic contribution, which is in the regime of non-perturbative quantum chromodynamics (QCD), entirely dominates the uncertainty of the SM value. That is the troublemaker in facing the current tensions of hadronic contribution among the experiment, the data-driven approach, and the lattice QCD simulation. The details will be explained in the following.

2 Hadronic contributions

The hadronic contribution to $(g-2)_\mu$ contains two parts: hadronic vacuum polarization and hadronic light-by-light, which are presented in Fig. 1.

*e-mail: x.l.ren@gsi.de

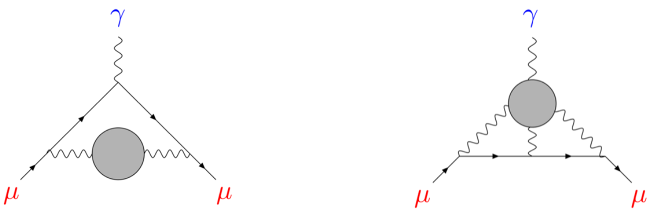

Figure 1. Hadronic contributions to the muon $g-2$. The left panel is HVP and the right panel denotes HLbL.

2.1 Hadronic vacuum polarization

HVP contribution begins at the second order of the fine-structure constant α and has been calculated up to α^4 using the data-driven approach [5]. Based on the analyticity and unitarity, the dispersion relations are employed to relate HVP to the experimental measurements. Specifically, dispersion integrals are constructed over the cross section of electron-positron annihilation, such as the leading order (LO) correction,

$$a_\mu^{\rm LO-HVP} = \frac{\alpha^2}{3\pi^2}\int_{m_\pi^2}^{\infty} ds \frac{K(s)}{s} R(s), \tag{4}$$

where the R-ratio is defined as $R(s) = \frac{\sigma^0(e^+e^-\to {\rm hadrons}(+\gamma))}{\sigma(e^+e^-\to\mu^+\mu^-)}$. The known kernel function $K(s)$ suppresses the contributions from high energies. As a result, the main contribution to HVP is from low energies, especially $\gtrsim 75\%$ from the $e^+e^- \to \pi^+\pi^-$ channel. Up to next-to-next-to-leading order, HVP presents a rather good convergence in the power of α and results in $a_\mu^{\rm HVP} = 6845(40)\times 10^{-11}$ [4]. Such large uncertainty of HVP is dominated by the accuracy of the cross section of $e^+e^- \to \pi^+\pi^-$ channel. Because there exists a long-standing tension between the BaBar [6] and KLOE [7] measurements, which gives a $2.9\,\sigma$ discrepancy on $(g-2)_\mu$. Furthermore, the most recent measurement by CMD-3 experiment [8] has made the situation more complicated: it disagrees with their earlier result of CMD-2 and also disagrees with all the existing experiments. Finally, this leads to the uncertainty up to 2-5% for the $e^+e^- \to \pi^+\pi^-$ cross section. This causes the challenge of the data-driven HVP approach because the $\pi^+\pi^-$ production cross section should have a $\sim 0.2\%$ overall systematical error to match the precision goal of FNAL-E989.

Besides the lattice QCD simulation provides an independent method to evaluate the LO-HVP from first principle. However, a $2.1\,\sigma$ discrepancy is observed for the LO-HVP between the sub-percent determination of BWM Collocation [9] and the data-driven result. Furthermore, if focusing on the intermediate-window contribution to the LO-HVP, different lattice groups achieve an impressive agreement. But there exists $3.8\,\sigma$ tension with the data-driven evaluation [10].

2.2 Hadronic light-by-light

HLbL contribution to the $(g-2)_\mu$, which involves the 4th-rank tensor of the light-by-light scattering amplitude, is more complicated than HVP. Fortunately, one does not need to achieve the same level of accuracy because HLbL is suppressed by a α/π factor compared to HVP. Therefore its accuracy is just needed around 10% to meet the precision goal of the FNAL experiment.

Nowadays, the dispersive relation is always employed to model-independently identify the HLbL contribution [11, 12]. The first step is to have the basis for the rank-4 polarization tensor, which satisfies Lorentz invariance and gauge invariance and is free of kinematic constraints. Then one needs to identify the cuts and intermediate states in the hadronic blob, as shown in Fig. 1. Due to the complications, a direct/simple approach is to formulate the dispersion relations for each intermediate state, e.g. pion (η, η') pole, pion (kaon) box, two-pion (two kaons, $\pi\eta$, $\eta\eta$,...) exchange, etc, as shown in Refs. [11–15]. Furthermore, the HLbL contribution can be calculated indirectly, such as the dispersion relation for Pauli form factor [16], the Schwinger sum rule to relate the photo-absorption cross section on the muon [17].

Based on the dispersion relation of HLbL, the light-by-light process can be related to the photon-photon fusion to hadrons $\gamma^{(*)}\gamma^{(*)} \to X$. In the experimental measurements of photon-photon fusion, the relevant transition form factors (TFFs) and partial wave amplitudes can be extracted. In this way, one can build a data-driven approach via the connection between HLbL and the experimental data of two-photon fusion. Currently, the magnitude of HLbL is estimated to be $92(19) \times 10^{-11}$ in the data-driven and dispersion approach [4]. The contributions from intermediate states, such as the pseudoscalar pole, pion (kaon) box, and pion-pion rescattering have been well determined with uncertainties below the precision goal. However, the estimation of the contribution from higher hadronic states in the energy region of $1 \sim 2$ GeV is challenging on both experimental and theoretical sides, and remains the major source of uncertainty.

Remark that the current situation of HLbL is better than HVP temporarily in comparison with the recent results of lattice calculations [18–21]. The HLbL contribution achieves a compatible result with uncertainties at the 20% level. But one would be advisable to keep in mind the complication of HLbL. If the ongoing tensions in HVP are solved, it would be intriguing to see how these solutions impact HLbL.

3 Photon-photon fusion

Now let's shift our attention to the processes of photon-photon fusion, which are the subprocesses of HLbL. A brief overview of the recent progress is provided below.

3.1 $\gamma^*\gamma^* \to \boldsymbol{P}$

For the light pseudoscalar-exchange contributions to HLbL, it can be factored as the space-like TFFs with the known weight functions [22]. The single and double virtual TFFs are the only inputs and can be determined via the $\gamma^*\gamma^* \to \boldsymbol{P}$ cross section. Currently, the π TFF is well determined, and the experimental results are consistent with the dispersion relation and the lattice simulations [15, 19, 23, 24]. While the η TFF is not well constrained due to the complicated $\eta - \eta'$ mixing. The tension is observed at the low Q^2 region between the Dyson-Schwinger equation analysis [25] and the lattice result [24]. Thus the measurement in this key region is necessary, and the dispersive analysis of $\eta^{(\prime)}$ TFF is also needed.

3.2 $\gamma^*\gamma^* \to \pi\pi, K\bar{K}, \pi\eta$

As to the two-pseudoscalar-exchange contribution to HLbL, the inputs of the data-driven approach are the partial wave amplitudes of the $\gamma^*\gamma^* \to \pi\pi, K\bar{K}, \pi\eta, ...$ reactions at arbitrary virtualities. From the experimental side, several groups have studied the processes of real-photon fusion $\gamma\gamma \to \pi\pi$. As to the $\pi\pi$ final states, the $\sigma/f_0(500)$, $f_0(980)$, $f_2(1285)$ resonances are relevant in the partial wave analysis. BSEIII preliminary results of $\gamma\gamma \to \pi\pi, \pi\eta, K^+K^-$

coupled channel analysis [26] was presented by M. Küßner in the conference. While for the single-tag measurement of photon-photon fusion, the experimental data is rather limited. The first measurement was carried out by Belle for $\gamma\gamma^* \to \pi^0\pi^0$ process [27] with the relative large Q^2. The BESIII is working on the $\gamma\gamma^* \to \pi^+\pi^-$ analysis [28], which provides a rather low region of Q^2 from 0.2 GeV^2 to 2 GeV^2 with the full helicity angle. On the theoretical side, the dispersive analysis of the $\gamma^{(*)}\gamma^{(*)} \to \pi\pi$ process has been studied as a single channel in the S wave [13], and then extended to the couple channel case by including $K\bar{K}$ contribution to formulate the helicity amplitudes of the S and D waves [29, 30]. A good description of the real-photon fusion data is observed. While these formulations still need to be validated by the upcoming single-virtual data of BESIII measurement. Furthermore, the dispersive study of $\gamma^*\gamma^* \to \pi\eta/K\bar{K}$ reaction [31] was presented by O. Deineka in the conference.

3.3 $\gamma\gamma \to \pi^+\pi^-\pi^0$ reaction

As mentioned before, one needs to better control the uncertainty from the axial vectors and tensors' contribution to HLbL around the energy region $1 \sim 2$ GeV. Below we list the major decay modes of the relevant resonances [32]:

	$a_1(1260)$	$f_1(1285)$	$f_1(1420)$	$a_2(1320)$
decay mode	$\pi\pi\pi$	$\eta\pi\pi$ $\pi\pi\pi\pi$	$K\bar{K}\pi$	$\pi\pi\pi$

In order to well control the $(g-2)_\mu$ contributions of these resonances, the detailed studies of the photon-photon fusion to 3π, $\eta\pi\pi$, $K\bar{K}\pi$, and 4π processes and confronting with the experimental data are necessary.

Towards this line, we investigated the $\gamma\gamma \to \pi^+\pi^-\pi^0$ process in Ref. [33] using a sophisticated phenomenological model. The existing experimental data, performed by the ARGUS [34] and L3 [35, 36] Collaborations, are rather old and have low statistics. In particular, as shown in Fig. 2, there exists a significant difference of cross section in the low-energy region, which is the most relevant for the HLbL contribution to a_μ. On the other hand, the previous theoretical studies of the $\gamma\gamma \to \pi^+\pi^-\pi^0$ are limited to the 3π threshold region using the linear

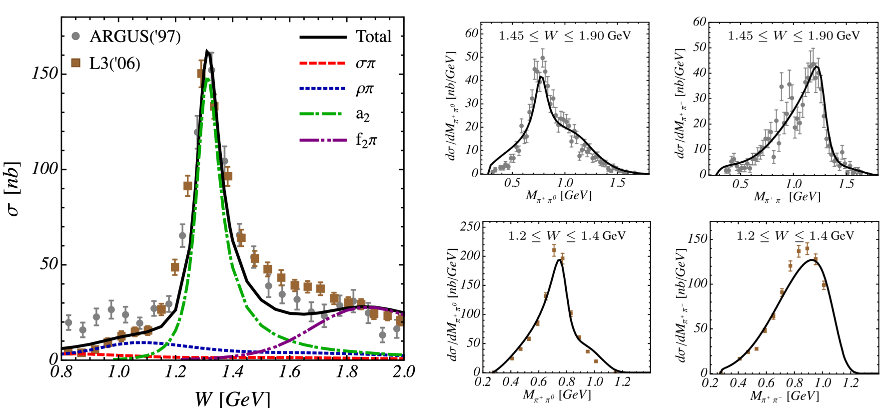

Figure 2. Total cross section and the two-pion invariant mass distributions for the $\gamma\gamma \to \pi^+\pi^-\pi^0$ process.

sigma model and chiral perturbation theory [37–39]. A sophisticated analysis to cover the low- and intermediate regions of ARGUS and L3 data is still missing.

Facing the forthcoming data from the BESIII measurement [40], we develop a phenomenological model of the real photon fusion process $\gamma\gamma \to \pi^+\pi^-\pi^0$ by taking into account the contributions of the $a_2(1320)$ resonance, the $\sigma/f_0(500)\pi^0$, $f_2(1270)\pi^0$, and $\rho^\pm\pi^\mp$ production channels. We employed the effective Lagrangians to describe the interaction vertices. The resulting amplitude is modified to have a correct high-energy behavior by considering the exchange of a Regge trajectory. Furthermore, the energy-dependent widths of the intermediate resonances ($a_2(1320)$, $f_2(1270)$, $\rho(770)$) are employed by including the Blatt-Weisskopf form factors. Among those contributions, we performed a careful investigation of $\gamma\gamma \to \rho^\pm\pi^\mp \to \pi^+\pi^-\pi^0$ channel by introducing the complete set of gauge invariant and Lorentz-covariant tensors for the $\gamma\gamma \to \rho^\pm\pi^\mp$ processes. Note that we have six effective couplings, five of which are determined by the decay widths of the relevant resonances. Thus, we only have one free parameter in our phenomenological model, which is fixed by the total cross section. The details can be seen in Ref. [33].

We found a rather good description of the total cross section and invariant mass distributions from ARGUS and L3 Collaborations, as shown in Fig. 2. It is worthy to mention that our model favors the smaller total cross section values of the L3 data at low energies. We also predicted the invariant mass distribution and the Dalitz plots for the total energies from 0.8 to 2.0 GeV, which will be studied by the forthcoming BESIII measurements of the $\gamma\gamma \to \pi^+\pi^-\pi^0$ reaction.

4 Summary and outlook

FNAL experiment has analyzed the data of the first three phases, leading to the precision of muon $g-2$ at an unprecedented level (~ 0.19 ppm). As expected, its precision will be sharpened to meet/beyond the 140 ppb goal after going through the measurement of the 4+5+6 phases in the following years. Such a result will be revisited in the J-PARC Muon $g-2$/EDM experiment [41], where a different strategy of measurement is under construction. Thus, the muon $g-2$ has provided a perfect playground to test the Standard Model and to investigate the new physics. This definitely requires tremendous effort to understand the hadronic contributions (HVP and HLbL) in the SM. In particular, one needs to solve the current tensions existing in HVP. The MUonE experiment at CERN [42] will provide new insight into this problem. As to the HLbL, the experimental measurements and the theoretical analyses of photon-photon fusion beyond two final states are really needed to pin down the uncertainties of the higher hadronic states' contributions.

Acknowledgments

It is a pleasure to thank the organizers for providing the chance to Kraków. This work is supported by the Deutsche Forschungsgemeinschaft (DFG), in part through the Research Unit (Project ID 458854507 - FOR 5327], and in part through the Cluster of Excellence ($PRISMA^+$ EXC 2118/1) within the German Excellence Strategy (Project ID 39083149).

References

[1] D. P. Aguillard *et al.* [Muon g-2], Phys. Rev. Lett. **131**, 161802 (2023)
[2] B. Abi *et al.* [Muon g-2], Phys. Rev. Lett. **126**, 141801 (2021)
[3] G. W. Bennett *et al.* [Muon g-2], Phys. Rev. D **73**, 072003 (2006)

[4] T. Aoyama, *et al.* Phys. Rept. **887**, 1-166 (2020)
[5] A. Kurz, T. Liu, P. Marquard and M. Steinhauser, Phys. Lett. B **734**, 144-147 (2014)
[6] J. P. Lees *et al.* [BaBar], Phys. Rev. D **86**, 032013 (2012)
[7] A. Anastasi *et al.* [KLOE-2], JHEP **03**, 173 (2018)
[8] F. V. Ignatov *et al.* [CMD-3], arXiv:2302.08834 [hep-ex].
[9] S. Borsanyi *et al.*, Nature **593**, 51-55 (2021)
[10] G. Colangelo *et al.*, Phys. Lett. B **833**, 137313 (2022)
[11] G. Colangelo, M. Hoferichter, M. Procura and P. Stoffer, JHEP **09**, 091 (2014)
[12] G. Colangelo, M. Hoferichter, M. Procura and P. Stoffer, JHEP **09**, 074 (2015)
[13] G. Colangelo, M. Hoferichter, M. Procura and P. Stoffer, JHEP **04**, 161 (2017)
[14] G. Colangelo, M. Hoferichter, M. Procura and P. Stoffer, Phys. Rev. Lett. **118**, 232001 (2017)
[15] M. Hoferichter, B. L. Hoid, B. Kubis, S. Leupold and S. P. Schneider, JHEP **10**, 141 (2018)
[16] V. Pauk and M. Vanderhaeghen, Phys. Rev. D **90**, 113012 (2014)
[17] F. Hagelstein and V. Pascalutsa, Phys. Rev. Lett. **120**, 072002 (2018)
[18] T. Blum, N. Christ, M. Hayakawa, T. Izubuchi, L. Jin, C. Jung and C. Lehner, Phys. Rev. Lett. **124**, 132002 (2020)
[19] E. H. Chao, R. J. Hudspith, A. Gérardin, J. R. Green, H. B. Meyer and K. Ottnad, Eur. Phys. J. C **81**, 651 (2021)
[20] E. H. Chao, R. J. Hudspith, A. Gérardin, J. R. Green and H. B. Meyer, Eur. Phys. J. C **82**, 664 (2022)
[21] T. Blum, N. Christ, M. Hayakawa, T. Izubuchi, L. Jin, C. Jung, C. Lehner and C. Tu, [arXiv:2304.04423 [hep-lat]].
[22] M. Knecht and A. Nyffeler, Phys. Rev. D **65**, 073034 (2002)
[23] I. Danilkin, C. F. Redmer and M. Vanderhaeghen, Prog. Part. Nucl. Phys. **107**, 20-68 (2019)
[24] A. Gérardin, W. E. A. Verplanke, G. Wang, Z. Fodor, J. N. Guenther, L. Lellouch, K. K. Szabo and L. Varnhorst, [arXiv:2305.04570 [hep-lat]].
[25] G. Eichmann, C. S. Fischer, E. Weil and R. Williams, Phys. Lett. B **797**, 134855 (2019)
[26] M. Küßner, Coupled channel partial wave analysis of two-photon reactions at BESIII, PhD Thesis, Ruhr-Universität Bochum (2022)
[27] M. Masuda *et al.* [Belle], Phys. Rev. D **93**, 032003 (2016)
[28] Y. Guo [BESIII], J. Phys. Conf. Ser. **1137**, 012008 (2019)
[29] I. Danilkin and M. Vanderhaeghen, Phys. Lett. B **789**, 366-372 (2019)
[30] M. Hoferichter and P. Stoffer, JHEP **07**, 073 (2019)
[31] I. Danilkin, O. Deineka and M. Vanderhaeghen, Phys. Rev. D **96**, 114018 (2017)
[32] R. L. Workman *et al.* [Particle Data Group], PTEP **2022**, 083C01 (2022)
[33] X.-L. Ren, I. Danilkin and M. Vanderhaeghen, Phys. Rev. D **107**, 054037 (2023)
[34] H. Albrecht *et al.* [ARGUS], Z. Phys. C **74**, 469-477 (1997)
[35] M. Acciarri *et al.* [L3], Phys. Lett. B **413**, 147-158 (1997)
[36] V. A. Shchegelsky, A. V. Sarantsev, A. V. Anisovich and M. P. Levchenko, Eur. Phys. J. A **27**, 199-205 (2006)
[37] S. L. Adler, B. W. Lee, S. B. Treiman and A. Zee, Phys. Rev. D **4**, 3497-3501 (1971)
[38] J. W. Bos, Y. C. Lin and H. H. Shih, Phys. Lett. B **337**, 152-156 (1994)
[39] P. Talavera, L. Ametller, J. Bijnens, A. Bramon and F. Cornet, Phys. Lett. B **376**, 186-192 (1996)

[40] C. F. Redmer [BESIII], EPJ Web Conf. **212**, 04004 (2019)
[41] Y. Sato [J-PARC E34], JPS Conf. Proc. **33**, 011110 (2021)
[42] G. Abbiendi *et al.*, Eur. Phys. J. C **77**, 139 (2017)